AGU PUBLICATIONS

Geophysical Research Letters

RESEARCH LETTER
10.1002/2016GL070216

Key Points:
- Magnetosonic waves can be a source of hydrogen band EMIC waves; the converse is also true
- Energy can be transferred from magnetosonic waves into EMIC waves via linear mode conversion
- Magnetosonic waves could be the source of EMIC waves in the inner belt and slot region

Correspondence to:
R. B. Horne,
R.Horne@bas.ac.uk

Citation:
Horne, R. B., and Y. Miyoshi (2016), Propagation and linear mode conversion of magnetosonic and electromagnetic ion cyclotron waves in the radiation belts, *Geophys. Res. Lett.*, *43*, 10,034–10,039, doi:10.1002/2016GL070216.

Received 28 JUN 2016
Accepted 8 SEP 2016
Accepted article online 15 SEP 2016
Published online 6 OCT 2016

Propagation and linear mode conversion of magnetosonic and electromagnetic ion cyclotron waves in the radiation belts

Richard B. Horne[1] and Yoshizumi Miyoshi[2]

[1]British Antarctic Survey, Cambridge, UK, [2]Institute for Space Earth Environment Research, Nagoya University, Nagoya, Japan

Abstract Magnetosonic waves and electromagnetic ion cyclotron (EMIC) waves are important for electron acceleration and loss from the radiation belts. It is generally understood that these waves are generated by unstable ion distributions that form during geomagnetically disturbed times. Here we show that magnetosonic waves could be a source of EMIC waves as a result of propagation and a process of linear mode conversion. The converse is also possible. We present ray tracing to show how magnetosonic (EMIC) waves launched with large (small) wave normal angles can reach a location where the wave normal angle is zero and the wave frequency equals the so-called crossover frequency whereupon energy can be converted from one mode to another without attenuation. While EMIC waves could be a source of magnetosonic waves below the crossover frequency, magnetosonic waves could be a source of hydrogen band waves but not helium band waves.

1. Introduction

Fast magnetosonic waves have been observed near the equator from as low as $L = 1.5$ to beyond $L = 8.0$ [*Russell et al.*, 1969; *Kasahara et al.*, 1994; *Zhima et al.*, 2015]. These waves are important as they can accelerate electrons up to MeV energies and help form the outer radiation [*Horne et al.*, 2007]. More recently, magnetosonic waves have been observed on the inner edge of the outer radiation belt and may be associated with butterfly-type electron distributions [*Li et al.*, 2016], although this is controversial [*Albert et al.*, 2016].

Electromagnetic ion cyclotron (EMIC) waves have also been observed in the magnetosphere, usually outside the plasmapause in a region extending out to the magnetopause [e.g., *Meredith et al.*, 2003]. EMIC waves are important for electron loss from the radiation belts [*Summers and Thorne*, 2003; *Albert*, 2003; *Miyoshi et al.*, 2008; *Kersten et al.*, 2014]. At lower L corresponding to the inner belt and slot region both EMIC waves and magnetosonic waves have been observed in overlapping regions between $L = 1.5$ and 2.5 by the Akebono satellite [*Kasahara et al.*, 1992, 1994]. On Akebono magnetosonic waves were referred to as type B emissions and extended to latitudes between $\pm 18^\circ$. Typically, the frequency range was 40–60 Hz.

It has been generally accepted that magnetosonic waves can be generated by a ring distribution in the proton and heavier ion distributions [e.g., *Horne et al.*, 2000] at energies of tens to hundreds of keV and that EMIC waves can be generated by a temperature anisotropy [e.g., *Sakaguchi et al.*, 2013]. However, unless there is a very large convection electric field, it is not clear how such ion distributions can form in the inner belt to generate waves observed near $L = 1.5$. The purpose of this paper is to consider the idea that waves such as magnetosonic waves generated in one region could propagate a large distance and provide the source of energy for another set of waves such as EMIC waves via linear mode conversion where different wave dispersion surfaces touch each other. Linear mode conversion has been proposed in other context, for example, to explain the emission of nonthermal continuum radiation emitted from the Earth [*Jones*, 1987; *Horne*, 1988, 1989], auroral kilometric radiation [*Oya and Morioka*, 1983], and wave emissions from Jupiter and Saturn [e.g., *Jones*, 1983, 1987]. As far as we are aware, it has not been applied to magnetosonic waves and EMIC waves associated with the radiation belts.

2. Dispersion Curves

To understand how energy can be transferred from one wave mode to another via linear mode conversion, it is instructive to study the dispersion curves. Figure 1a shows an example of the dispersion curves for wave

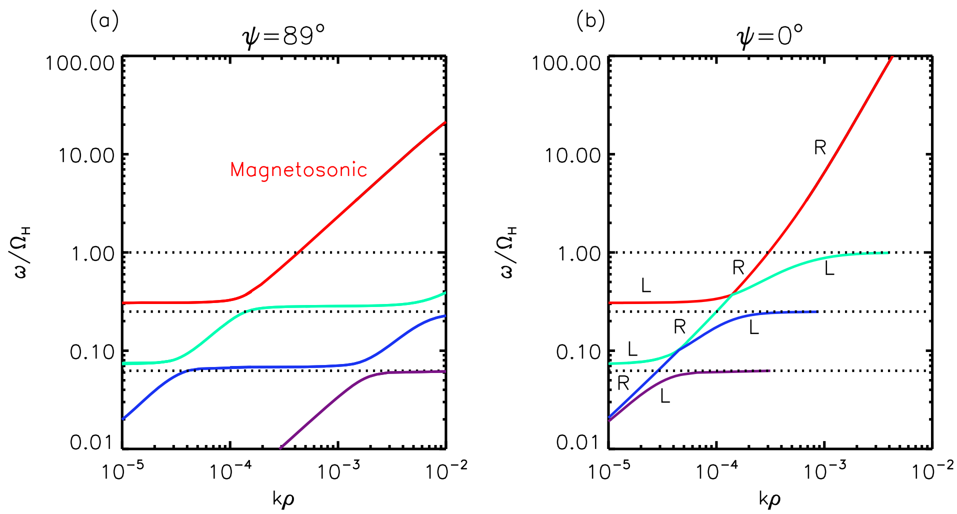

Figure 1. Dispersion curves for waves propagating in cold plasma for (a) $\psi = 89°$ and (b) $\psi = 0°$ with respect to the magnetic field direction. The wave frequency is normalized to the proton cyclotron frequency Ω_H, and the proton gyroradius ρ is set to $\rho = 1$ m. The color coding refers to the same dispersion surface, the R (L) refer to right (left)-hand polarization.

propagation at an angle of 89° with respect to the magnetic field direction. Magnetosonic waves can be generated above the proton cyclotron frequency (Ω_H) on this branch[e.g., *Horne et al.*, 2000]. The dispersion curves here were calculated for a cold plasma using the HOTRAY code [*Horne*, 1989] using the diffusive equilibrium plasma density model [*Inan and Bell*, 1977] and a dipole magnetic field. The dispersion curves are shown for $L = 1.5$ at the equator for $f_{pe}/f_{ce} = 3.31$ and an ion composition of 91.4% H^+, 7.1% He^+ and 1.5% O^+. (The temperature, density, and ion composition at the base $r_b = 1100$ km of the diffusive equilibrium model were $T_{DE} = 5000$ K, $N_b = 1.5 \times 10^{10}$ el m^{-3}, 44% H^+, 8% He^+, and 48% O^+ with a plasmapause at $L_p = 4.0$ with a half width of $W = 0.6$. The other parameters are the same as in *Inan and Bell* [1977]).

The dispersion curves are actually surfaces that vary with frequency and wave normal angle, as does the wave polarization. For example, the red curves in Figure 1 are for the same dispersion surface. At large wave normal angles (Figure 1a) the waves correspond to linearly polarized *X* mode waves which extend up in frequency to the lower hybrid resonance frequency, whereas for parallel propagation (Figure 1b) the waves are right-hand polarized above the crossover frequency in a multi-ion plasma and left-hand polarized below. At intermediate angles the waves are a mixture of right-hand—linear or left-hand—linear polarization. The green, blue, and black curves show wave dispersion surfaces at lower frequencies.

It is interesting to note that when waves are observed by satellites below Ω_H, they are generally referred to as EMIC waves, or sometimes hydrogen, helium, or oxygen band EMIC waves, whereas when waves are observed above Ω_H, they may be referred to as magnetosonic waves. The red curves in Figure 1 show that it may be possible for magnetosonic waves to propagate into a region where $\omega < \Omega_H$, and vice versa. This is discussed below.

It is important to note that the dispersion surfaces in Figure 1a remain separate from each other. In contrast, Figure 1b shows that for parallel propagation ($\psi = 0°$) the dispersion curves touch each other at two particular frequencies, known as the crossover frequencies [*Budden*, 1985; *Horne and Thorne*, 1993]. The dispersion curves only touch for parallel propagation, at any finite angle of propagation the curves remain separate and distinct. Theory shows that during propagation the waves must remain on the same dispersion branch. This means that the wave polarization can change during propagation, for example, as a result of changes in the magnetic field strength and hence crossover frequency, but the waves cannot change mode. The exception to this rule is that wave energy can be transferred from one wave mode to another without attenuation at the frequency where the two dispersion surfaces touch [*Budden*, 1985]. Thus, magnetosonic waves, generated above Ω_H, if they can propagate into a region where $\omega < \Omega_H$ can transfer energy into hydrogen band EMIC waves if the wave frequency equals the crossover frequency and $\psi = 0°$, i.e., where the red and green curves touch. Similarly, energy could be transferred between EMIC waves at the crossover frequency where the green

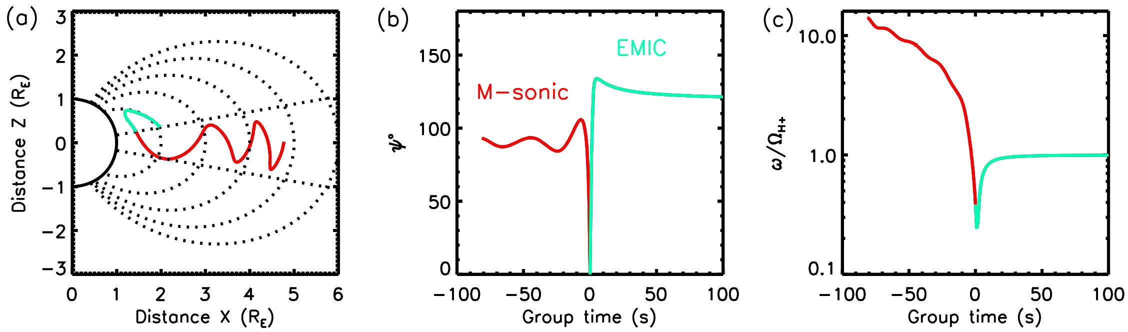

Figure 2. (a) A magnetosonic wave (red) as a source of an EMIC wave (green). Energy can be transferred from the (b) magnetosonic wave into the EMIC wave when $\psi = 0°$ and the (c) wave frequency equals the crossover frequency.

and blue curves touch. The process is analogous to energy conversion between the LO and Z mode when the wave frequency equals the plasma frequency $f = f_{pe}$ [e.g., *Jones*, 1987] and between the whistler mode and Z mode when $f_{pe} < f_{ce}$. Wave energy can still be exchanged if there is a small mismatch in frequency or in the angle of propagation, but in this case energy is attenuated, and the process is more efficient if there is a large density gradient present [*Budden*, 1985].

3. Ray Tracing

In order to test the idea of mode conversion, it is necessary to consider where the waves are generated and test whether they can propagate into a region where mode conversion can take place. Here we first consider the case where magnetosonic waves are the source of EMIC waves and whether they can access the highest crossover frequency. We use the density model described above and ray tracing in a cold plasma using the HOTRAY code. Details of the growth and propagation in a hot plasma are left for future work.

Magnetosonic waves can be generated by a proton ring distribution in the vicinity of the plasmapause and are usually observed near the magnetic equator with very large wave normal angles. Figure 2a shows an example of a magnetosonic wave (red curve) launched from $L = 4.77$ at a latitude of $\lambda = 0.28°$ with $\psi = 93.0°$ at a frequency $f = 61.89$ Hz. The initial frequency corresponds to $\omega/\Omega_H = 14.18$ and is consistent with the generation of magnetosonic waves between the harmonics of the proton cyclotron frequency. Ray tracing is started with $t < 0$ so that the ray will reach the mode conversion point at $t = 0$. The wave propagates toward the Earth in the meridian plane and is confined in latitude to approximately $\lambda < 10°$, as illustrated by the dotted lines. The plasma density and magnetic field gradients refract the wave so that the wave normal angle passes through 90° 5 times (Figure 2b). The normalized wave frequency (Figure 2c) generally decreases as the ray propagates closer to the Earth and drops below $\omega/\Omega_H = 1$. In the region where $\omega/\Omega_H < 1$ the wave normal angle is large but gradually decreasing, and hence, the wave polarization is a mixture of right-hand linear polarization. As the ray continues propagating, it reaches a location where the wave frequency equals the crossover frequency with $\psi = 0°$. This corresponds to $t = 0$. Thus, contrary to the expectation that the wave normal angle is always close to 90°, magnetosonic waves can be refracted so that the wave normal angle becomes small for part of the propagation path. At this location, which is approximately $L = 1.5$ $\lambda = 10°$ wave energy can be transferred from magnetosonic waves into EMIC waves without attenuation via linear mode conversion [*Budden*, 1985]. The green curve shows the propagation of a hydrogen band EMIC wave launched from the mode conversion region with $\psi = 0°$. The wave "reflects" in the Northern Hemisphere and on return the wave frequency approaches the proton cyclotron frequency Ω_H with ψ large. In this case ray tracing is stopped as one would expect the EMIC wave to be absorbed by proton cyclotron damping. Thus, mode conversion could result in heating the ion distribution.

Ray tracing shows that magnetosonic waves at other frequencies can access the crossover frequency with $\psi = 0°$ over a wide range of L shells and latitudes (not shown). Since the crossover frequency depends on the magnetic field strength and the ion composition, and these tend to decrease with radial distance, energy conversion at lower frequencies should take place farther from the Earth.

To demonstrate that the process can operate in reverse and that EMIC waves could be a source of magnetosonic waves, Figure 3 shows an example of an EMIC wave launched from $L = 1.52$ with $\lambda = 0.11°$,

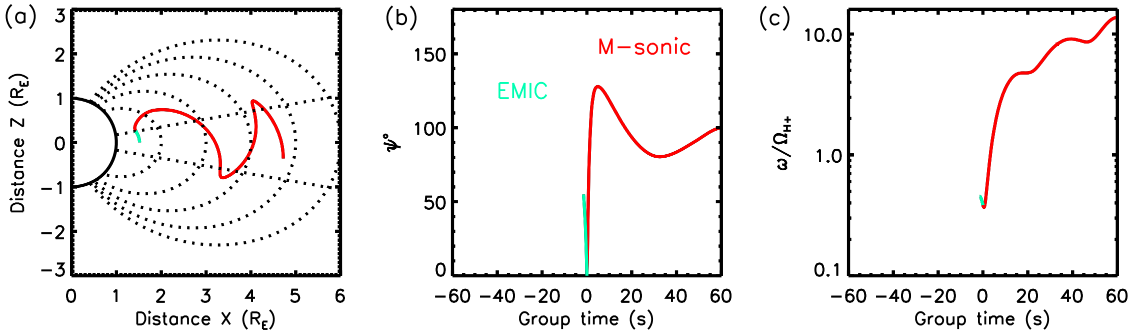

Figure 3. An EMIC wave (green) as a source of a magnetosonic wave (red).

$\psi = 54.89°$, $\omega/\Omega_H = 0.46$, and $t < 0$. In this case the wave propagates only a short distance along the field line, and wave growth should be possible just above the equator where the wave normal angle is small. The wave reaches the crossover frequency at $t = 0$ with $\psi = 0°$ (Figures 3b and 3c) whereupon energy conversion into magnetosonic waves can take place. The red curve shows a magnetosonic wave launched with $\psi = 0°$ propagating away from the mode conversion region toward larger *L*. The ray is stopped after propagating for 60 s.

4. Discussion

Magnetosonic waves have been detected over a wide range of *L* shells from the inner to the outer radiation belt [*Russell et al.*, 1969; *Kasahara et al.*, 1994]. Strong magnetosonic waves have been observed by the Van Allen Probes mission at the inner edge of the outer radiation belt [*Li et al.*, 2016] with much higher amplitudes than previously detected. Magnetosonic waves can be generated by a proton ring distribution with very large wave normal angles, and such a ring distribution can form as a result of the energy dependence in the transport and loss of protons around the magnetosphere [e.g., *Chen et al.*, 2010]. Under these conditions we suggest that magnetosonic waves could be the source of EMIC waves.

The proton energy usually associated with the growth of EMIC waves via Doppler-shifted cyclotron resonance is typically in the region of tens to hundreds of keV. Protons in this energy range do not usually penetrate into the slot region unless there is a very large convection electric field, which can be the case during storms. The EMIC waves observed by Akebono were observed for a range of K_p, but most often for $K_p = 2$ [*Kasahara et al.*, 1992, 1994]. The generation of EMIC waves by energetic protons could therefore take place after a storm during the time it takes for the ring current to decay, which can be several days. Thus, we suggest that under these conditions EMIC waves could be a source of magnetosonic waves in the inner radiation belt and slot region as a result of energy conversion at the crossover frequency.

While energy conversion between magnetosonic waves and EMIC waves can take place in either direction, there is an important difference. In principle EMIC waves at low *L* could be a source of magnetosonic waves at larger *L*, but magnetosonic waves could only provide a source of hydrogen band waves. It seems very unlikely that magnetosonic waves could provide a source of helium band waves since this would require additional mode conversion between hydrogen band waves and helium band waves at the lower crossover frequency which would require special propagation conditions.

In this paper we have not considered hot plasma effects such as the generation of magnetosonic waves by proton ring distributions or EMIC waves by a temperature anisotropy or wave damping. These effects are left for future work. However, our ray tracing is consistent with the growth and propagation magnetosonic waves at large wave normal angles and with the confinement of the waves to within a few degrees of the magnetic equator. It is also consistent with the growth of EMIC waves with small wave normal angles near the magnetic equator. Other magnetic field and density gradients could reduce the latitudinal spread of magnetosonic waves and help confine them more closely to the equator.

Magnetosonic waves can cause electron acceleration up to MeV energies via Landau resonance [*Horne et al.*, 2007]. This would tend to reduce the amplitude of the waves, but the electron flux is usually very low at such high energies so the reduction in wave power may be small. EMIC waves, on the other hand, cause electron loss from the radiation belts. The conversion of wave energy from magnetosonic waves into EMIC waves may thus pose an interesting question as to how much energy goes into the acceleration of radiation belt electrons and how much goes into electron loss.

5. Conclusions

We have shown by ray tracing that fast magnetosonic waves could provide the source of energy for EMIC waves observed in the inner belt and slot region as a result of inward propagation and linear mode conversion at the crossover frequency. We have also shown that the converse is true and that EMIC waves could provide a source of magnetosonic waves which propagate outward from the inner belt and slot region. Theory shows that energy conversion is unattenuated when the wave frequency equals the crossover frequency, but if there is any mismatch in frequency or angle of propagation, then energy is attenuated, and the process is more efficient when there is a large density gradient present [*Budden*, 1985].

Energy conversion via linear mode conversion can take place in either direction, but while EMIC waves could provide a source for magnetosonic waves, magnetosonic waves can only provide a source for hydrogen band EMIC waves and are very unlikely to be a source of helium band waves as this would require additional mode conversion and special propagation conditions.

The range of frequencies where linear mode conversion can take place is determined by the maximum and minimum of the crossover frequency. Hot plasma effects may restrict the frequency range even further. However, since the crossover frequency depends on the magnetic field strength and the ion composition which both tend to drop with increasing distance, mode conversion is likely to take place at larger L for lower frequencies.

We suggest that one way to test the origin of the waves is to examine experimentally the wave polarization. In the hydrogen band, just below the proton cyclotron frequency and above the crossover frequency, if the wave polarization is mainly linear with a right-hand polarized component, then the waves are more likely to originate from magnetosonic waves via propagation effects; on the other hand, if they have a left-hand polarized component, they are more likely to be generated by Doppler-shifted cyclotron resonance. A survey of the wave power in both magnetosonic and EMIC waves could also be used to test the linear mode conversion idea.

Acknowledgments
The research leading to these results has received funding from the European Union Seventh Framework Programme (FP7/2007-2013) under grant agreement 606716 (SPACESTORM), STFC grant ST/M00130X/1, and the Natural Environment Research Council. Y. Miyoshi is supported by Grants-in-Aid for Scientific Research (15H05815 and 15H05747) of the Japan Society for the Promotion of Science (JSPS). The data used to generate the plots in this paper can all be found in the references.

References

Albert, J. M. (2003), Evaluation of quasi-linear diffusion coefficients for EMIC waves in a multispecies plasma, *J. Geophys. Res.*, *108*, 1249, doi:10.1029/2002JA009792.

Albert, J. M., M. J. Starks, R. B. Horne, N. P. Meredith, and S. A. Glauert (2016), Quasi-linear simulations of inner radiation belt electron pitch angle and energy distributions, *Geophys. Res. Lett.*, *43*(6), 2381–2388, doi:10.1002/2016GL067938.

Budden, K. G. (1985), *The Propagation of Radio Waves*, Cambridge Univ. Press, New York.

Chen, L., R. M. Thorne, V. K. Jordanova, and R. B. Horne (2010), Global simulation of magnetosonic wave instability in the storm time magnetosphere, *J. Geophys. Res.*, *115*, A11222, doi:10.1029/2010JA015707.

Horne, R. B. (1988), Ray tracing of electrostatic waves in a hot plasma and its application to the generation of terrestrial myriametric radiation, *Geophys. Res. Lett.*, *15*, 553–556.

Horne, R. B. (1989), Path-integrated growth of electrostatic waves: The generation of terrestrial myriametric radiation, *J. Geophys. Res.*, *94*, 8895–8909.

Horne, R. B., and R. M. Thorne (1993), On the preferred source location for the convective amplification of ion cyclotron waves, *J. Geophys. Res.*, *98*, 9233–9247.

Horne, R. B., G. V. Wheeler, and H. St. C. K. Alleyne (2000), Proton and electron heating by radially propagating fast magnetosonic waves, *J. Geophys. Res.*, *105*, 27,597–27,610.

Horne, R. B., R. M. Thorne, S. A. Glauert, N. P. Meredith, D. Pokhotelov, and O. Santolík (2007), Electron acceleration in the Van Allen radiation belts by fast magnetosonic waves, *Geophys. Res. Lett.*, *34*, L17107, doi:10.1029/2007GL030267.

Inan, U. S., and T. F. Bell (1977), The plasmapause as a VLF wave guide, *J. Geophys. Res.*, *82*, 2819–2827.

Jones, D., W. Calvert, D. A. Gurnett, and R. L. Huff (1987), Observed beaming of terrestrial myriametric radiation, *Nature*, *328*, 391–395.

Jones, D. (1983), Source of saturnian myriametric radiation, *Nature*, *306*(5942), 453–456.

Jones, D. (1987), Io plasma torus and the source of jovian narrow-band kilometric radiation, *Nature*, *327*, 492–495.

Kasahara, Y., A. Sawada, M. Yamoto, I. Kimura, S. Kokubun, and K. Hayashi (1992), Ion cyclotron emissions observed by the satellite Akebono in the vicinity of the magnetic equator, *Radio Sci.*, *27*, 347–362.

Kasahara, Y., H. Kenmochi, and I. Kimura (1994), Propagation characteristics of the ELF emissions observed by the satellite Akebono in the magnetic equatorial region, *Radio Sci.*, *29*, 751–767.

Kersten, T., R. B. Horne, S. A. Glauert, N. P. Meredith, B. J. Fraser, and R. S. Grew (2014), Electron losses from the radiation belts caused by EMIC waves, *J. Geophys. Res. Space Physics*, *119*, 8820–8837, doi:10.1002/2014JA020366.

Li, J., et al. (2016), Formation of energetic electron butterfly distributions by magnetosonic waves via Landau resonance, *Geophys. Res. Lett.*, *43*, 3009–3016, doi:10.1002/2016GL067853.

Meredith, N. P., R. M. Thorne, R. B. Horne, D. Summers, B. J. Fraser, and R. R. Anderson (2003), Statistical analysis of relativistic electron energies for cyclotron resonance with EMIC waves observed on CRRES, *J. Geophys. Res.*, *108*(A6), 1250, doi:10.1029/2002JA009700.

Miyoshi, Y., K. Sakaguchi, K. Shiokawa, D. Evans, J. Albert, M. Connors, and V. Jordanova (2008), Precipitation of radiation belt electrons by EMIC waves, observed from ground and space, *Geophys. Res. Lett.*, *35*, L23101, doi:10.1029/2008GL035727.

Oya, H., and A Morioka (1983), Observational evidence of Z and L-O mode waves as the origin of auroral kilometric radiation from the Jikiken (EXOS-B) satellite, *J. Geophys. Res.*, *88*, 6189–6203.

Russell, C. T., R. E. Holzer, and E. J. Smith (1969), OGO 3 observations of ELF noise in the magnetosphere, 1. Spatial extent and frequency of occurrence, *J. Geophys. Res.*, *74*, 755–777.

Sakaguchi, K., Y. Kasahara, M. Shoji, Y. Omura, Y. Miyoshi, T. Nagatsuma, A. Kumamoto, and A. Matsuoka (2013), Akebono observations of EMIC waves in the slot region of the radiation belts, *Geophys. Res. Lett.*, *40*, 1–5, doi:10.1002/2013GL058258.

Summers, D., and R. M. Thorne (2003), Relativistic electron pitch-angle scattering by electromagnetic ion cyclotron waves during geomagnetic storms, *J. Geophys. Res.*, *108*(A4), 1143, doi:10.1029/2002JA009489.

Zhima, Z., L. Chen, H. Fu, J. Cao, R. B. Horne, and G. Reeves (2015), Observations of discrete magnetosonic waves off the magnetic equator, *Geophys. Res. Lett.*, *42*, 9694–9701, doi:10.1002/2015GL066255.